BMC Medical Imaging

RESEARCH

Open Access

Cerebral morphometric alterations predict the outcome of migraine diagnosis and subtyping: a radiomics analysis

Tong-Xing Wang[1†], Xiao-Bin Huang[1†], Tong Fu[1], Yu-Jia Gao[1], Di Zhang[1], Lin-Dong Liu[1], Ya-Mei Zhang[1], Hai Lin[2], Jian-Min Yuan[2], Cun-Nan Mao[1*] and Xin-Ying Wu[1*]

Abstract

Background This study aimed to identify cerebral radiomic features related to migraine diagnosis and subtyping into migraine with aura (MwA) and migraine without aura (MwoA) and to develop predictive models based on these markers.

Method We retrospectively analyzed MR imaging from 88 migraine patients (32 MwA and 56 MwoA) and 49 healthy control subjects (HCs). Features representing the gray matter morphometry and diffusion properties were extracted from participants via histogram analysis. These features were put through an all-relevant feature selection procedure within cross-validation loops to identify features with significant discriminative power for migraine diagnosis and subtyping. Based on the selected features, the predictive ability of the random forest models constructed from the previous sample was tested in an independent sample of 30 patients (10 MwA) and 17 HCs.

Result No overall differences in total brain volume or gray matter volume were revealed between patients and HCs, or between MwA and MwoA (all *P* values > 0.05). Six features significantly differed between patients and HCs for migraine diagnosis, and four features distinguished MwA from MwoA for subtyping (all *P* values < 0.001). Four features were significantly correlated with headache severity score (all *P* values < 0.01). Based on these relevant features, the random forest models achieved accuracies of 80.9% in distinguishing patients from HCs and 76.7% in differentiating MwA from MwoA in the testing cohort.

Conclusion Our findings suggest cerebral radiomic alterations in migraine patients may potentially serve as a biomarker to assist in migraine diagnosis and subtyping, contributing to personalized treatment strategy.

Clinical trial number Not applicable.

Keywords Migraine with aura, Migraine without aura, T1-weighted MR imaging, Diffusion tensor imaging, Radiomics

[†]Tong-Xing Wang and Xiao-Bin Huang contributed equally to this work.

*Correspondence:
Cun-Nan Mao
maocunan@163.com

Xin-Ying Wu
rebeccahxt@163.com
[1]Department of Radiology, Nanjing First Hospital, Nanjing Medical University, No. 68, Changle Road, Nanjing, Jiangsu Province 210006, China
[2]Central Research Institute, United Imaging Healthcare, Shanghai, China

Background

Migraine is a primary neurologic disorder featured by complex manifestations beyond just headache. It affects over 1 billion people worldwide and has negative influences on both personal and socioeconomic levels [1]. It is majorly categorized into migraine without aura (MwoA) and migraine with aura (MwA). MwoA is considered the common type of migraine, while MwA has specific symptomatic features. Migraine aura could manifest as visual, sensory, speech and/or language, motor, brainstem, and retinal symptoms [2, 3]. Compared to MwoA, patients with MwA experience fewer headache attacks but longer-lasting headache attack duration (including the time of aura symptoms and the headache attack). Patients with MwA also exhibit a higher level of anxiety, which may more significantly affect their life quality [1, 3]. Additionally, MwoA may respond to acute treatments more quickly than MwA since there is no aura phase delaying the onset of headache [4]. Moreover, MwA patients have a higher risk of aura-related ischemic stroke and cardiovascular disease than MwoA [5, 6]. Therefore, accurate migraine subtyping, particularly for aura, based on an understanding of the disease mechanism, is preferred for aura-specific therapy, which may help to reduce the risk of aura-related vascular events [7]. However, diagnosis of migraine, as well as migraine subtyping into MwA and MwoA, is for now based solely on clinical criteria, which lack objective evidence and provide limited pathophysiological information. Especially, given the diverse clinical manifestations of MwA, the incidence of misdiagnosis in clinical practice remains relatively high. For instance, visual aura symptoms may be transient, and the clinical presentation can resemble other neurological conditions. Research has demonstrated that current criteria are insufficient for accurately diagnosing MwA in some cases due to overlapping features with other disorders, making it prone to misdiagnosis [8]. Clinical assessment alone cannot fully address the complexity of MwA symptoms, which may vary widely in presentation. Therefore, it is essential to develop methodologies that address these limitations and enable more accurate and objective diagnostic capabilities. To better understand the complex pattern of migraine manifestation and make optimal patient-specific decisions, neuroimaging markers that would improve migraine diagnosis and subtyping are highly desirable.

Neuroimaging markers reflecting morphological alteration of gray matter in migraine patients are of great importance in explaining the possible mechanisms of migraine [9, 10]. Structural changes in gray matter are fundamental to variations in brain function and metabolism. In addition, trigemino-thalamo-cortical pathway is considered an important possible theory of MwoA and is widely reported to be associated with regional gray matter (GM) changes [10–13]. Cortical spreading depression (CSD), characterized by propagating depolarization neurons and glia in cortical gray matter with a breakdown of normal ionic gradient that translates into neurologic symptoms, has been considered as the prominently possible theory for migraine aura [2]. The topologic folding feature of the gray matter of the human gyrencephalic brain (highly folded), involving negative and positive Gaussian curvature, is strongly related to CSD progress [14]. In previous studies, gray matter macromorphological alterations in migraine patients have been demonstrated as changes in volume, cortical thickness, local gyrification index, and cortical surface area [15–17]. The indices of diffusion tensor imaging (DTI) imply the microstructural changes in gray matter, including the loss of myelinated fibers passing through gray matter, tissue compaction and gliosis, the loss of certain dendrite connection, the breakdown of microstructural barriers to diffusion, ferritin-bound iron concentration, and so on [18, 19]. Gray matter structural integrity also relates to neuronal activity, which evokes local cerebral blood flow increase through neurovascular coupling (NVC), a process of great importance in CSD [20]. Therefore, information about macro- and micro-structural variations in gray matter in migraine patients is of great importance for better understanding the underlying mechanisms.

Radiomic features applied to machine learning models provide promising results with quantitative imaging information and play an increasingly important role in diagnosis prediction, treatment response, and prognosis [21]. The random forest algorithm builds multiple of decision trees during training and outputs the mode for classification or the mean prediction of the individual trees, showing superior performance in neuroimaging feature capturing compared to traditional machine learning methodology with satisfactory accuracies in previous imaging studies [22, 23]. The robustness in handling high-dimensional data and the ability to measure feature importance without extensive parameter tuning made the random forest algorithm ideal for our study. We applied rigorous feature selection to minimize overfitting and improve the model generalizability, followed by cross-validation to ensure stability and reliability. We plan to introduce improvements in imaging feature selection and validation that enhance the random forest algorithm performance in neuroimaging feature extraction of migraine. Machine learning approaches were applied in the studies of migraine neuroimaging biomarker derived from functional MRI with promising accuracy [24, 25], highlighting its diagnostic value for migraine [26]. However, subtle morphometric radiomic characteristics derived from brain gray matter in migraine patients, which are fundamentally associated with

trigemino-thalamo-cortical pathway and CSD mechanism theories, remain indispensable.

Thus, the present study applied the random forest algorithm and cross-validation to capture the morphometric radiomic features of migraine in the training group, aiming to detect potential brain morphological markers with diagnostic value for migraine for classifying MwA and MwoA. The performance of the radiomic analysis would be further evaluated using external testing group.

Methods

Participants and clinical assessments

The human study was approved by the local ethics committee of our hospital (No.KY20200301-16), and written informed consent was obtained from each participant. Patients were recruited from the neurological wards. Ninety-seven patients were diagnosed with episodic migraine according to the third version of the International Classification of Headache Disorders (ICHD-3) [3]. Diagnostic criteria for migraine without aura and migraine with aura were then used to classify patients into MwoA and MwA groups. Patients with probable migraine, additional neurological disease other than migraine, severe head injury, drug abuse, use of preventive medications, other major medical illness, brain vascular disease, or hydrocephalus, as well as those who failed to complete the MR examination, were excluded from the study. In the end, 88 migraine patients were enrolled into the training group, including 56 MwoA and 32 MwA (22 with visual/retinal symptom, eight with sensory symptom, four with language symptom and one with motor symptom) patients. Forty-nine healthy control subjects (HCs) matched to patients in respect to age, sex and education were also enrolled into this study. They were recruited from the local population and had no personal or family history of migraine, or any other types of headaches. To minimize hormonal influences on cortical excitability, all female subjects were included at mid-cycle and excluded if pregnant or breastfeeding. All migraine patients and HCs were right-handers according to self-report. The age and gender of both HCs and migraine patients, as well as the disease duration and migraine frequency of all migraine patients, were collected according to self-reports. All patients completed a headache severity score assessment via a numeric pain rating scale. Fisher's test for gender and two-tailed t-tests for continuous variables were conducted in the comparisons between groups. In addition, another group of migraine patients was recruited as an external testing cohort from the neurological wards. The same inclusion and exclusion criteria for MwA and MwoA and the same clinical evaluations were applied to these patients. Finally, 30 migraine patients (10 MwA) and 17 HCs were included in the testing group.

Image acquisition and preprocessing

All participants in the training and testing groups were scanned at a 3.0T MRI scanner. (uMR 780, United Imaging Healthcare, Shanghai, China) during the interictal phase of migraine episodes. The MR examination contained a protocol of high-resolution three-dimensional T1-weighted MR images (T1WI, a MATRIX sequence, resolution $1 \times 1 \times 1$ mm [3], TI = 800ms, TR/TE = 8.1 ms/3.7 ms, slices = 170, flip angle = 10°, acquisition matrix = 256×100, Field of View (FOV) = 256 mm × 256 mm, bandwidth = 250, accelerator factor = 3.5), and diffusion-weighted images (echo-planar imaging, 64 weighted directions and 2 b0 images, b = 1000 s/mm^2, resolution $2 \times 2 \times 2$ mm [3], TE/TR = 85ms/12080ms, acquisition matrix = 128×100, FOV = 256 mm × 256 mm, bandwidth = 1630, accelerator factor = 2.0, flip angle = 90°/180°).

The DTI data were preprocessed using the Functional Magnetic Resonance Imaging of the Brain software (FMRIB Software Library, FSL; University of Oxford, London). Motion and eddy current distortions were corrected using the "eddy" script. A brain mask of the non-diffusion-weighted image was created using the BET in FSL. Diffusion tensors were calculated using the "dtifit" script to obtain the following four diffusion parameters: fractional anisotropy (FA), mean diffusivity (MD), axial diffusivity (AD), and radial diffusivity (RD).

The extraction of radiomic features

All T1WIs were processed using the script of recon-all in Freesurfer with the Desikan-Killiany-Tourville atlas. A total of 2338 shape-related features (including mean, standard deviation, skew, and kurtosis of local thickness, mean curvature, convexity, geodesic depth, and travel depth) representing gray matter morphometry were extracted using the Mindboggle software, as detailed in the previous studies [27].

According to the Brainnetome atlas, which parcellates the brain into 210 cortical and 36 subcortical subregions [28], four types of histogram metrics (mean, standard deviation, skew, and kurtosis) were extracted from each of four parameter maps (FA, MD, AD and RD). A total of 1968 features representing the diffusion properties of gray matter regions were extracted from each participant's DTI data.

Feature selection and model construction

There were 88 and 30 migraine patients in the training and testing groups, with nearly the same percentage of MwoA and MwA patients ($P > 0.5$ in a chi-squared test). The percentages of patients and HCs in the training and testing groups were also not significantly different ($P > 0.5$ in a chi-squared test). Feature selection and model construction were performed simultaneously only

in the training group. To select radiomic features with significant discriminative power for migraine diagnosis or MwA identification, all features were put into an all-relevant feature selection procedure within cross-validation loops using the random forest algorithm (Fig. 1 and Supplementary Figure S1). We repeated 100 times of 10-fold cross validation, which resulted in a total of 1000 training-validation cycles. In detail, the 10-fold cross validation involves dividing the dataset into 10 almost equal parts, using nine parts for training and the remaining one part for validation at a time, and repeating this process 10 times with each part serving as the validation set once. For each iteration, a random forest classifier was constructed from the training set using the randomForest package with default parameters in MATLAB (MathWorks, Natick, MA). The performance of the classifier

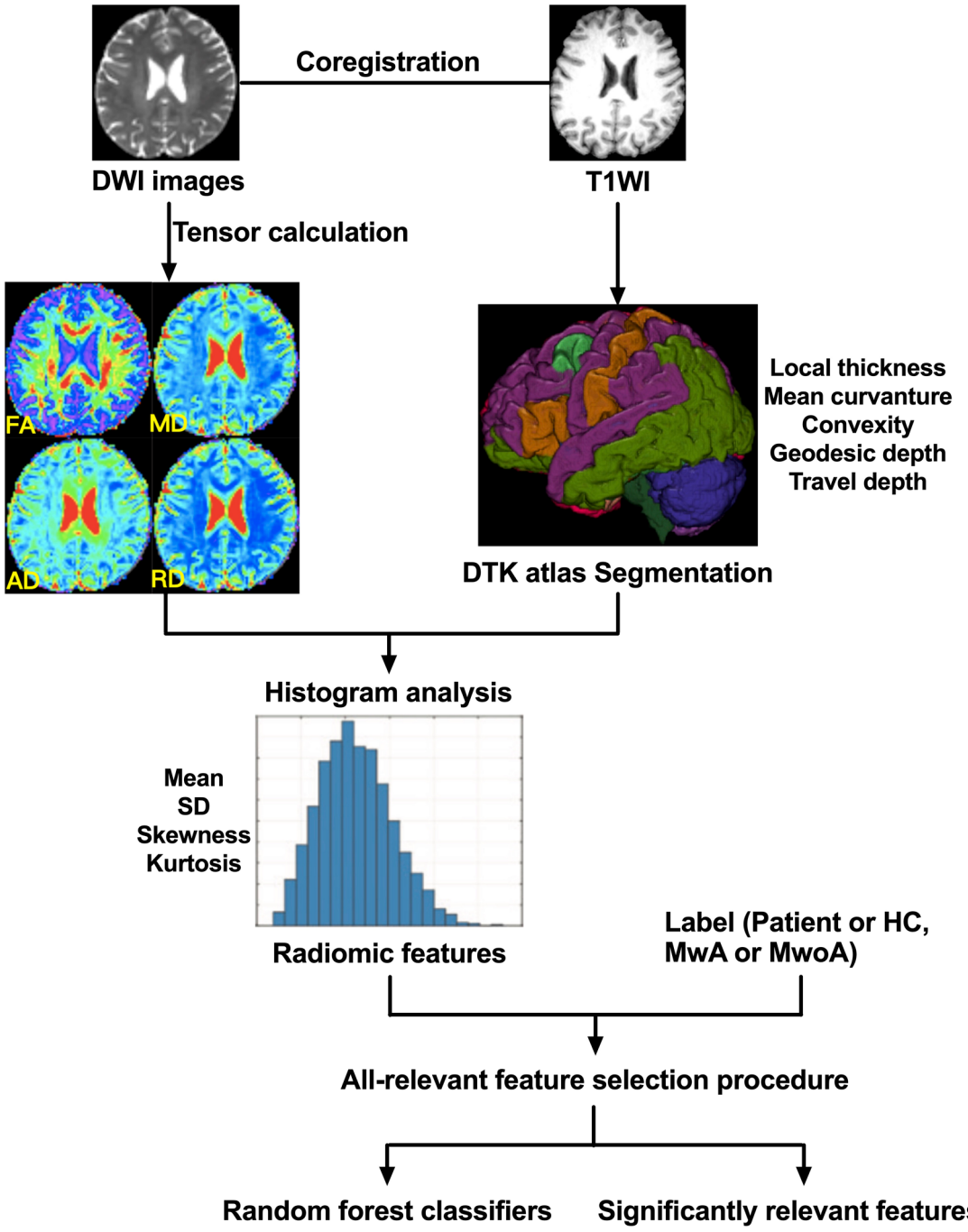

Fig. 1 The flowchart of an all-relevant feature selection procedure within 10-fold cross-validation loops, to identify features with significant discriminative power for classification

Table 1 The demographic and clinical characteristics and macroscopic cerebral volume measurements of all participants

	MwA (*n* = 32)	MwoA (*n* = 56)	HC (*n* = 49)	Patients versus HCs *p*-value[a]	MwA versus MwoA *p*-value[a]
Age (years)	35.4 ± 12.1	37.0 ± 8.9	37.4 ± 8.9	0.56	0.48
Gender (Male/Female)	7/25	11/45	16/33	0.11[b]	0.80[b]
Disease duration (years)	11.8 ± 8.7	14.4 ± 8.8	NA	NA	0.19
Frequency (days per month)	4.1 ± 4.0	5.4 ± 6.6	NA	NA	0.35
Headache severity score	6.0 ± 1.4	4.3 ± 1.2	NA	NA	< 0.01
Cortical gray matter volume (mm^3)	432553.6 ± 22598.4	440723.2 ± 38454.2	432320.8 ± 25861.6	> 0.1	> 0.1
Subcortical gray matter volume (mm^3)	59687.6 ± 3591.8	61099.4 ± 5889.6.8	59370.4 ± 6388.5	> 0.1	> 0.1
Total gray matter volume (mm^3)	582754.2 ± 31497.8	602319.5 ± 49657.5	592792.6 ± 44949.8	> 0.1	> 0.1
Total brain volume (mm^3)	1209944.5 ± 209687.7	1273486.6 ± 231421.3	1277152.6 ± 261605.0	> 0.1	> 0.1

HC: Healthy controls, MwA: migraine patients with aura, MwoA: migraine patients without aura, NA: not applicable

Values are represented as the mean ± standard deviation, except for the gender distribution

[a]Unless otherwise indicated, p values were calculated with two-tailed t-tests

[b]p Value was obtained using a chi-squared test

Table 2 Significantly relevant features to discriminate migraine patients and healthy controls

Selection frequency (%) *	Feature description	Patients	Healthy controls	*p*-value
92.1	Skewness of convexity in thalamus	-0.72 ± 0.12	-0.56 ± 0.08	< 0.001
91.3	Mean of local thickness in postcentral sulcus	2.15 ± 0.12	2.07 ± 0.11	< 0.001
88.4	Kurtosis of mean diffusivity in insula	5.54 ± 1.27	6.40 ± 1.44	< 0.001
86.1	Kurtosis of mean curvature in postcentral	-0.27 ± 0.45	-0.48 ± 0.31	0.004
82.1	Skewness of travel depth in caudal middle frontal	-0.47 ± 0.15	-0.31 ± 0.11	< 0.001
80.7	Standard deviation of fractional anisotropy in inferior parietal	0.18 ± 0.04	0.21 ± 0.06	< 0.001

* Defined as the number of iterations in which the feature was selected divided by the total number of iterations performed

was evaluated in the validation set. Among all iterations, different subsets of features were selected based on different folds. The selection frequency of each feature was defined as the number of iterations in which the feature was selected divided by the total number of iterations.

A permutation test (permuted 1000 times) was applied to identify the features with significantly higher selection frequency than random values as migraine-related or MwA-related selections. The statistical results were corrected for multiple comparisons using the False Discovery Rate (FDR) method for the corresponding p-value. Based on the identified features, the final random forest models were constructed from the training group and were further evaluated in the testing group.

After the feature selection, group comparisons and correlations with the headache severity score were performed for all the features with significant discriminative power using two-tailed t-tests and Pearson's correlation analysis in MATLAB (MathWorks, Natick, MA). *Because men typically exhibit an 11–13% larger brain volume than women, we accounted for it by including gender and age covariates in all volumetric analyses.*

Results

Demographic and clinical characteristics and macroscopic volumetric measurements

The demographic and clinical characteristics, as well as macroscopic cerebral volume measurements of all participants were summarized in Table 1 and Supplementary Table 1. There were no significant differences in age, gender, disease duration (time since diagnosis), or migraine frequency between MwA and MwoA patients, using a chi-squared test for gender and two-tailed t-tests for continuous variables (all P values > 0.05). The MwA group showed a higher headache severity score compared to the MwoA group ($P < 0.01$). Moreover, there were no significant differences in total brain volume or gray matter volume between patients and HCs, nor between MwA and MwoA (all P values > 0.05), *with gender and age included as covariates.*

Significantly relevant radiomic features

In constructing the random forest classifiers to discriminate between migraine patients and HCs, six features were identified as significantly relevant to classification by the permutation test (all P values < 0.01, Table 2; Fig. 2). Compared to HCs, the six features identified in patients included lower skewness of convexity in thalamus, higher mean of local thickness in postcentral sulcus,

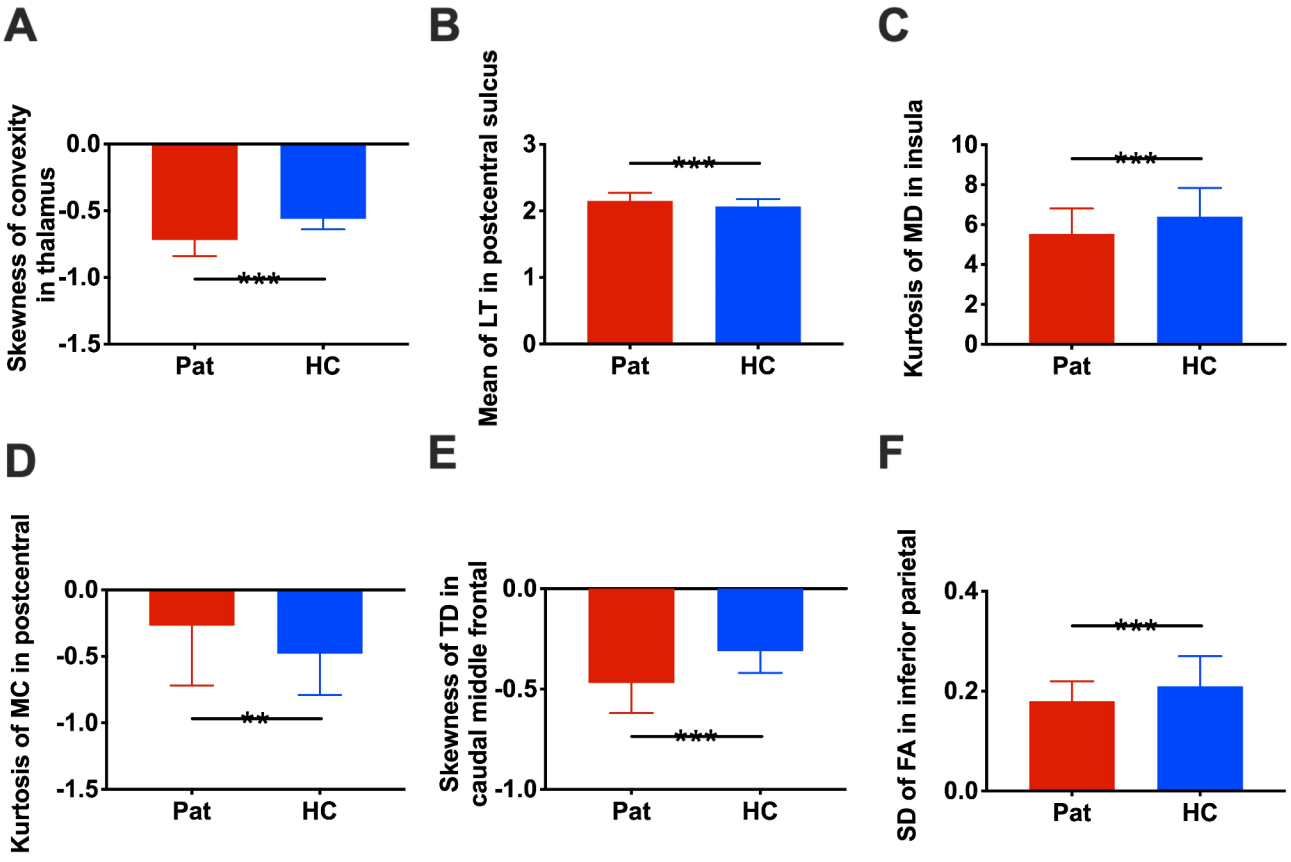

Fig. 2 Six identified connectivity features to discriminate migraine patients from HCs, using the all-relevant feature selection algorithm. These features were listed as follows: the skewness of convexity in thalamus (**A**) the mean of local thickness (LT) in postcentral sulcus (**B**) the kurtosis of mean diffusivity (MD) in insula (**C**) the kurtosis of mean curvature (MC) in postcentral (**D**) the skewness of travel depth (TD) in caudal middle frontal (**E**) the standard deviation (SD) of fractional anisotropy (FA) in inferior parietal (**F**). They all showed significant differences between patients and HC. Statistical significance is indicated by asterisks (***, $P<0.001$; **, $P<0.01$)

Table 3 Significantly relevant features to discriminate migraine patients with and without aura

Selection frequency (%) *	Feature description	MwA	MwoA	*p*-value
91.7	Mean of travel depth in caudal middle frontal	6.56 ± 0.69	6.04 ± 0.54	< 0.001
90.1	Standard deviation of fractional anisotropy in postcentral	0.14 ± 0.02	0.16 ± 0.02	< 0.001
85.3	Mean of convexity in lateral occipital	-3.26 ± 0.26	-2.94 ± 0.29	< 0.001
81.2	Mean of fractional anisotropy in thalamus	0.37 ± 0.02	0.39 ± 0.03	0.004

MwA: migraine patients with aura, MwoA: migraine patients without aura

* Defined as the number of iterations in which the feature was selected divided by the total number of iterations performed

lower kurtosis of mean diffusivity in insula, higher kurtosis of mean curvature in postcentral, lower skewness of travel depth in caudal middle frontal, and lower standard deviation of fractional anisotropy in inferior parietal. Four features showed significant differences between MwA and MwoA, relevant to subtyping, including higher mean of travel depth in caudal middle frontal, lower standard deviation of fractional anisotropy in postcentral, lower mean of convexity in lateral occipital, and lower mean of fractional anisotropy in thalamus in MwA compared to MwoA (all P values < 0.01, Table 3; Fig. 3). Several features were significantly correlated with the headache severity score in patients (Fig. 4), including the mean of local thickness in postcentral sulcus ($r=0.35$, $P=0.009$), kurtosis of mean curvature in postcentral ($r=-0.38$, $P=0.004$), mean of travel depth in caudal middle frontal ($r=0.45$, $P<0.001$) and mean of fractional anisotropy in thalamus ($r=-0.37$, $P=0.005$).

Prediction outcomes in the testing group

Six potential radiomic markers of migraine patients and four markers of MwA patients were identified after the feature selection procedure in the training group. On basis of these markers, the random forest models constructed from the training group achieved accuracies of 80.9% to identify migraine patients from HCs and 76.7%

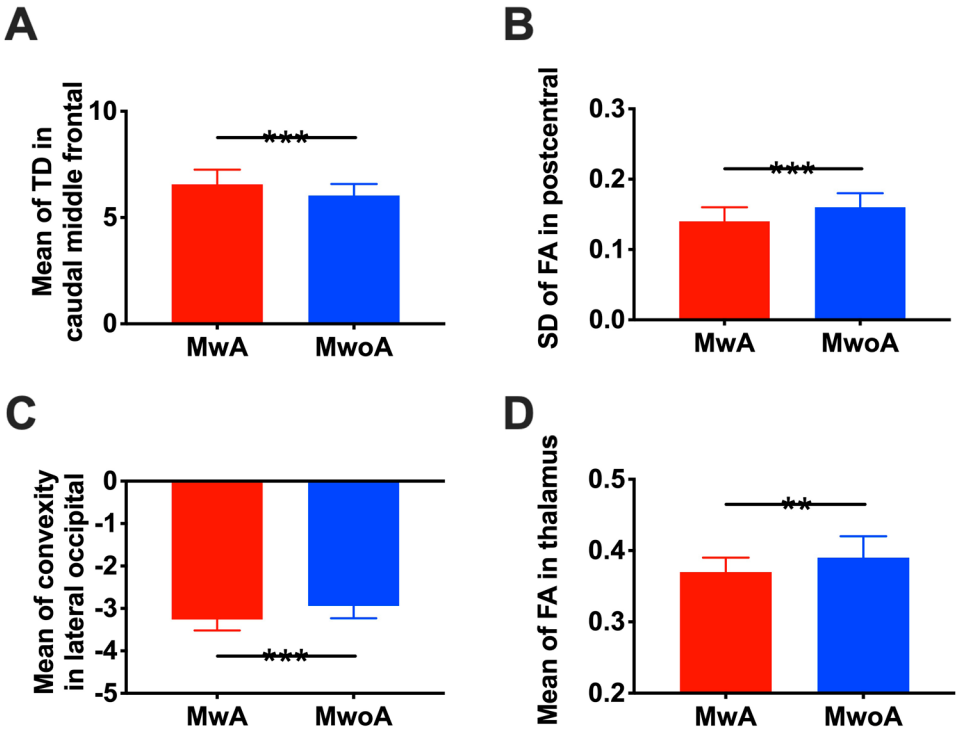

Fig. 3 Four identified connectivity features to discriminate MwA from MwoA patients, using the all-relevant feature selection algorithm. These features were listed as follows: the mean of travel depth (TD) in caudal middle frontal (**A**) the standard deviation (SD) of fractional anisotropy (FA) in postcentral (**B**) the mean of convexity in lateral occipital (**C**) the mean of FA in thalamus (**D**). They all showed significant differences between MwA and MwoA patients. Statistical significance is indicated by asterisks (***, $P < 0.001$; **, $P < 0.01$)

in discriminating MwA patients from the MwoA in the testing group.

Discussion

This study applied radiomic analysis to identify quantitative imaging features related to migraine diagnosis and subtyping into MwA and MwoA. Both macro- and micro- cerebral gray matter morphologic alterations were detected in migraine patients, including shape-related features of thalamus, postcentral and caudal middle frontal, postcentral sulcus, and the diffusion index of insula and inferior parietal. The accuracy of the six features to diagnose migraine exceeded 80% in the external sample validation test. Meanwhile, the shape-related features of caudal middle frontal and lateral occipital, along with the diffusion index of postcentral and thalamus, significantly contributed to differentiating MwA from MwoA with accuracy exceeded 75% in the external validation test.

Consistent to previous studies, no overall difference in total gray matter volume was revealed between our MwA and MwoA groups [29], nor between our migraine group and HCs [30]. The cerebral shape-related index alterations in our migraine patients, including lower negative values of skewness of convexity in thalamus and skewness of travel depth in caudal middle frontal, higher mean local cortical thickness in postcentral sulcus, and negative value of kurtosis of mean curvature in postcentral, showed focal cerebral topological feature consistent with previous studies. In a study on neuroanatomical signatures, Chou et al. also found increased cortical thickness in left postcentral sulcus in migraine patients [31]. However, there are also contradictory results demonstrating decreased cortical thickness in postcentral sulcus in migraine patients [16, 29, 31]. The discrepant results of focal cortical thickness suggest maladaptive changes linked to cortical plasticity related to the chronic progression of headache attacks, such as the frequency of headaches, and may be affected by cortical folding involving ion imbalances [10]. Another morphological feature of postcentral, the higher negative kurtosis of the mean curvature, was also found in our migraine group, indicating the curvature of postcentral has more spatial variation. Similar to our findings, an increased gyrification index in left postcentral gyrus was reported in a group of 32 MwoA patients [32]. Cerebral curvature alteration has also been reported in chronic and episodic migraine [33]. It is argued that the alterations of the cortex curvature index in migraine may be associated with neuro-hyperactivity and ion gradient fluctuation [14]. Hyperneural activity and increased amplitude of low-frequency fluctuation (ALFF) signals were detected in postcentral gyrus, encoding pain intensity in chronic migraine patients [34,

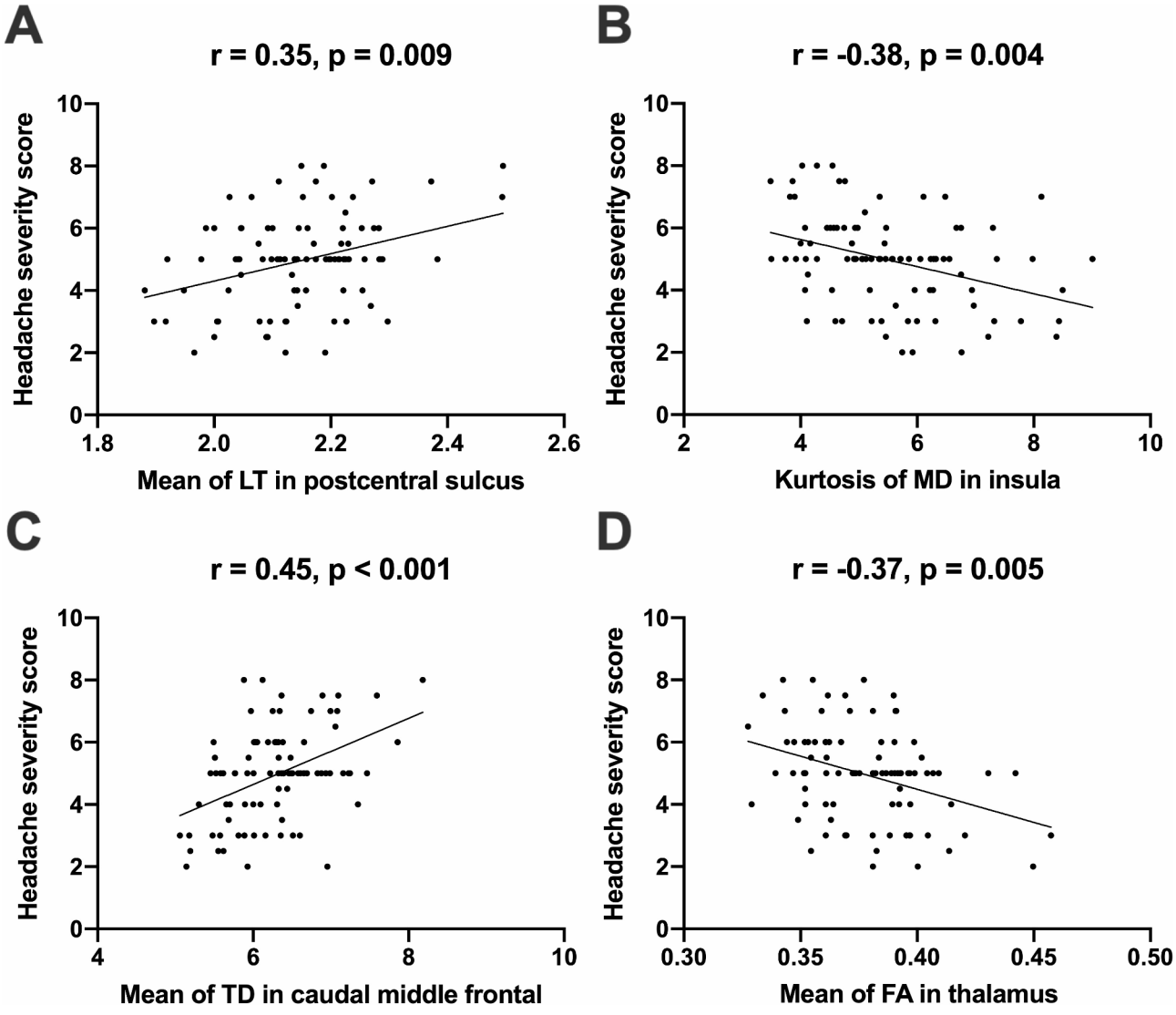

Fig. 4 Relationship between the disease severity and identified connectivity features. Significant correlations were revealed between the headache severity score and mean of local thickness (LT) in postcentral sulcus, kurtosis of mean diffusivity (MD) in insula, mean of travel depth (TD) in caudal middle frontal, and mean of fractional anisotropy (FA) in thalamus among all patients (**A-D**, all *P* values < 0.01, after FDR correction)

35]. Previous studies have demonstrated no significant difference in thalamus volume between migraine and healthy controls, but subtle volume alteration in subthalamus regions [13, 36]. Similarly, we did not find any brain volume alteration in migraine, but we did observe lower negative skewness of convexity in thalamus. Alterations in cerebral blood flow were detected in both thalamus and postcentral gyrus in migraine in our previous study [37]. Both thalamus and postcentral are critical components of the trigemino-thalamo-cortical pathway, which is considered an important headache circuit in migraine [7]. Thus, the morphological alteration detected in our results may also contribute to the understanding of migraine mechanism.

The alteration of distribution metrics of diffusion indices (mean diffusivity in insula and fractional anisotropy in inferior parietal) in our patients suggests microstructural changes in gray matter. Similarly, lower grey matter density in the right inferior parietal was also observed in migraine, and a decreased local gyrification index in the left superior parietal was detected in a cohort of seventy-two pediatric MwoA patients [15]. The structural alteration of insula in migraine patients has been widely reported [16, 32], and it is the fundamental factor in neural function, both functional and structural connectivity, and metabolism. Mean diffusivity (MD) reflects the average water molecule diffusion in all directions, while fractional anisotropy (FA) reflects the directionality of diffusion. The diffusion index is primarily used to

estimate the integrity of white matter. Alterations in MD and FA in gray matter have been previously reported in migraine [38]. The changes of distribution metrics of diffusion indices in our results are not visually observable but significantly contribute to differentiating migraine patients from HCs. The alteration of MD has been reported as a potentially earlier biomarker than volume in reflecting the microstructural integrity and organizational changes in gray matter [18]. Altered FA values in gray matter may reflect the composition and orientation of myelin, as well as the changes in glial cell density and orientation. Additionally, FA in gray matter has been reported to correlate with iron concentrations, possibly due to the clustering effect of ferritin in vivo, which increases magnetic inhomogeneity [19]. The gray matter microstructural changes in insula and inferior parietal in our migraine group may correspond to their important roles in the salience network and pain modulation [39].

Taken together, the macro- and micro-cerebral morphometric features, along with diffusion indices of gray matter from our results, may provide diagnostic tools for classifying migraine into MwA and MwoA (Fig. 2), which also adds imaging radiomics information of gray matter alteration of migraine subtypes. In previous studies, cerebral alterations in caudal middle frontal and occipital in MwA were reported, including cortical depth, cortical thickness, cerebral blood flow, and functional connectivity [37, 40–42]. Our results highlighted the higher absolute values of mean convexity in lateral occipital and mean travel depth in caudal middle frontal in MwA compared to MwoA, indicating greater variation in curvature, which represents more special variation. Cerebral cortex special variation affects the initiation, propagation, and cessation of extracellular K^+ waves in CSD, widely recognized as the underlying pathophysiological mechanism of MwA [14]. The alterations in the SD of FA in postcentral and mean FA in the thalamus in MwoA were greater than those in MwA, demonstrating gray matter microstructure differences between MwoA and MwA. The difference in microstructure of the postcentral and thalamus between MwoA and MwA may be attributed to different pain modulation pathways [2].

In terms of clinical symptoms, the headache severity score showed correlations with the morphological features. The postcentral sulcus is a prominent structure in somatosensory processing and an important component in the trigemino-thalamo-cortical pathway, which has been widely reported as a possible mechanism underlying migraine [7]. The positive correlation between headache severity and cortical thickness of postcentral sulcus might be attributed to the hyperexcitability of neurons under the condition of pain in migraine. The caudal middle frontal plays a role in cognitive function and emotion processing in migraine [2, 7]. The fluctuation of curvature (travel depth) in the caudal middle frontal may influence cognitive and emotional processing, which could exacerbate the perception of pain and contribute to higher headache severity. Moreover, these positive correlations might indicate an interaction between sensory processing, emotion, and cognitive factors in migraine. As headache severity increases, the brain might engage sensory processing (via the postcentral sulcus) and emotional and cognitive processing (via the caudal middle frontal area) to a greater level. The negative correlations between headache severity and mean FA in thalamus, as well as the kurtosis of MD in insula, imply that as headache severity increases, the microstructure of insula and thalamus become less variable in terms of water molecule diffusion. This might reflect a form of plasticity and adaptive response, where the microstructures become more uniform in the face of repeated or severe headaches in migraine [43–45]. In our previous study, hyper-perfusion in postcentral sulcus also worsened the headache (positively correlated), while hypo-perfusion in thalamus alleviated the headache (negatively correlated) [37]. The results of our two studies (same cohorts) suggest that the multiple index alterations of the same brain area possibly interact with each other and contribute to clinical manifestations. Also, the microstructural alteration may have interactions with the vasculature, together affecting the headache severity.

The cost-benefit trade-off of using neuroimaging biomarkers in migraine diagnosis is significant, with MRI costs ranging from $500 to $1,000 in North America and Europe. However, these costs are justified by the potential benefits. Early-stage neuroimaging insights are critical for accurate diagnosis and timely intervention, which can prevent fatal complications such as ischemic stroke or cardiovascular disease [5, 6]. Neuroimaging biomarkers offer objective, reproducible results that clinical assessments may miss, potentially reducing misdiagnosis and improving patient outcomes in the long term. Thus, the costs of neuroimaging may be outweighed by its ability to guide effective therapy and prevent severe consequences.

This study has some limitations. Compared with the training sample, the sample size of MwA in the testing group was relatively small. Due to the relatively limited sample size in a single cohort, our diagnosis models need to be further tested and confirmed with more samples from multiple institutions. We did not account for potential confounders such as smoking, alcohol consumption, and Body Mass Composition, which could affect the interpretation of our findings and we will consider incorporating these variables more comprehensively in future studies. There exists heterogeneity in migraine with aura, which is probably associated with the pathophysiological mechanism of aura. However, we did not categorize our MwA group into specific subtypes, such as typical aura

migraine, brainstem aura migraine, hemiplegic migraine, or retinal migraine. In our further studies, we will focus on collecting and investigating various subtypes of the MwA group to explore potentially distinct neuroimaging biomarkers and their clinical implications. We applied cross-validation to assess the generalizability of our model, it is still possible that optimistic performance estimates may result from overfitting. Our radiomics analysis identified possible macro- and micro-morphological feature differences between MwA and MwoA, which are valuable, but the mathematic indices alone can't provide direct explanation of the clinical symptoms or the underlying mechanisms. One possible strategy to improve the interpretability and relevance of radiomic indices is to integrate radiomic data with clinical information, such as patient history, or to apply multimodal data fusion. The cohort results of our research, including the cerebral blood flow alterations [37] and functional and structural connectivity [46], along with present findings, provide fundamental preliminary work for further multimodal data fusion studies to bridge the gap between radiomics findings and clinical practice. These approaches could help align radiomics findings with clinical saturation, creating more comprehensive models that better capture migraine's complexity and enhancing their application in personalized diagnostics and treatments. Since migraine is a dynamic neurological disorder, a larger group of patients with continuous longitudinal follow-up studies are still needed to provide insights into how these imaging markers evolve and whether they correlate with clinical assessments.

Conclusions

The main finding of this study is that the cerebral morphologic feature derived from the MR imaging radiomics analysis aligns with existing theories and previous reports by distinguishing migraine from HC and revealing subtle brain microstructural differences between MwA and MwA that are not visually detectable. We applied MRI radiomics-based analysis to identify imaging biomarkers, which could potentially aid clinicians in accurately diagnosing migraine and MwA with objective, non-invasive evidence. Despite the challenges, our study holds promise for broader application across diverse patient populations and clinical settings, representing a valuable step towards better understanding the disease patterns of migraine, various aura symptoms, and unclear underlying physio-pathological mechanisms.

Abbreviations

AD	Axial diffusivity
ALFF	Amplitude of low-frequency fluctuation
CSD	Cortical spreading depression
DTI	Diffusion tensor imaging
FA	Fractional anisotropy
FDR	False discovery rate
FOV	Field of view
FSL	FMRIB software library
GM	Gray matter
HCs	Healthy control subjects
ICHD-3	The third version of the international classification of headache disorders
MD	Mean diffusivity
MwA	Migraine with aura
MwoA	Migraine without aura
NVC	Neurovascular coupling
RD	Radial diffusivity
SD	Standard deviation
T1WI	T1-weighted MR images
TE	Echo time
TR	Repetition time

Supplementary Information

The online version contains supplementary material available at https://doi.org/10.1186/s12880-025-01645-w.

Supplementary Material 1

Supplementary Material 2

Acknowledgements

We would like to thank all participants of this study.

Author contributions

Conception and design: XYW; (II) Administrative support: XYW and CNM; (III) Provision of study materials or patients: TXW, LDL, and CNM; (IV) Collection and assembly of data: TXW, YJG, DZ, LDL and CNM; (V) Data analysis and interpretation: TF, YMZ, HL and JMY; (VI) Drafting the manuscript: TXW and XBH. (VII) Revising manuscript for intellectual content: TXW, XBH， TF, XDY, CNM and XYW; (VIII) Final approval of manuscript: All authors.

Funding

This research was supported by Nanjing Science and Technology Planning Project (No. 202002056), Natural Science Foundation of Jiangsu Province (BK20230155), and 2023 Nanjing Medical Association Radiology Branch Medical Imaging Artificial Intelligence Special Research Fund Project (No. 11).

Data availability

The datasets used and analyzed during the current study are available from the corresponding author on reasonable request.

Declarations

Ethical approval

The authors are accountable for all aspects of the work in ensuring that questions related to the accuracy or integrity of any part of the work are appropriately investigated and resolved. The study was conducted in accordance with the Declaration of Helsinki (as revised in 2013). The study was approved by the Human Research Ethics Committee of the Nanjing First Hospital (Number KY20200301-16) and written informed consent was provided by the participants.

Consent for publication

Not applicable.

Competing interests

The authors declare no competing interests.

Received: 5 November 2024 / Accepted: 18 March 2025
Published online: 07 April 2025

References

1. Ashina M, Katsarava Z, Do TP, Buse DC, Pozo-Rosich P, Özge A, Krymchantowski AV, Lebedeva ER, Ravishankar K, Yu S, Sacco S, Ashina S, Younis S,

Steiner TJ, Lipton RB. Migraine: epidemiology and systems of care. Lancet. 2021;397:1485–95.
2. Goadsby PJ, Holland PR, Martins-Oliveira M, Hoffmann J, Schankin C, Akerman S. Pathophysiology of migraine: A disorder of sensory processing. Physiol Rev. 2017;97:553–622.
3. Tepper SJ. Editorial: international classification of headache disorders, 3rd edition, beta version. Headache. 2013;53:1381–2.
4. Ferrari MD, Goadsby PJ, Burstein R, Kurth T, Ayata C, Charles A, Ashina M, van den Maagdenberg AMJM, Dodick DW, Migraine. Nat Rev Dis Primers. 2022;8(1):2.
5. Chen D, Willis-Parker M, Lundberg GP. Migraine headache: is it only a neurological disorder? Links between migraine and cardiovascular disorders. Trends Cardiovasc Med. 2020;30:424–30.
6. Yemisci M, Eikermann-Haerter K. Aura and stroke: relationship and what we have learnt from preclinical models. J Headache Pain. 2019;20(1).
7. Burstein R, Noseda R, Borsook D. Migraine: multiple processes, complex pathophysiology. J Neurosci. 2015;35:6619–29.
8. Thomsen AV, Ashina H, Al-Khazali HM, Rose K, Christensen RH, Amin FM, Ashina M. Clinical features of migraine with aura: a REFORM study. J Headache Pain. 2024;25:22.
9. Nyholt DR, Borsook D, Griffiths LR. Migrainomics-identifying brain and genetic markers of migraine. Nat Reviews Neurol. 2017;13:725–41.
10. Tolner EA, Chen S, Eikermann-Haerter K. Current Understanding of cortical structure and function in migraine. Cephalalgia. 2019;39:1683–99.
11. Faragó P, Tóth E, Kocsis K, Kincses B, Veréb D, Király A, Bozsik B, Tajti J, Párdutz Á, Szok D, Vécsei L, Szabó N, Kincses ZT. Altered resting state functional activity and microstructure of the white matter in migraine with aura. Front Neurol. 2019;10:1–8.
12. Kim YE, Kim MK, Suh SI, Kim JH. Altered trigeminothalamic spontaneous low-frequency oscillations in migraine without aura: a resting-state fMRI study. BMC Neurol. 2021;21:1–9.
13. Shin KJ, Lee HJ, Park KM. Alterations of individual thalamic nuclei volumes in patients with migraine. J Headache Pain. 2019;20(1).
14. Kenny A, Plank MJ, David T. The effects of cerebral curvature on cortical spreading depression. J Theor Biol. 2019;472:11–26.
15. Ashina S, Bentivegna E, Martelletti P, Eikermann-Haerter K. Structural and functional brain changes in migraine. Pain Therapy. 2021;10:211–23.
16. Guarnera A, Bottino F, Napolitano A, Sforza G, Cappa M, Chioma L, Pasquini L, Rossi-Espagnet MC, Lucignani G, Figà-Talamanca L, Carducci C, Ruscitto C, Valeriani M, Longo D, Papetti L. Early alterations of cortical thickness and gyrification in migraine without aura: a retrospective MRI study in pediatric patients. J Headache Pain. 2021;22:1–13.
17. Messina R, Rocca MA, Valsasina P. Cortical abnormalities in patients with migraine: A Surface- based analysis. Radiology. 2013;268:170–80.
18. Henf J, Grothe MJ, Brueggen K, Teipel S, Dyrba M. Mean diffusivity in cortical Gray matter in Alzheimer's disease: the importance of partial volume correction. NeuroImage: Clin. 2018;17:579–86.
19. Rulseh AM, Keller J, Tintěra J, Kožíšek M, Vymazal J. Chasing Shadows: what determines DTI metrics in Gray matter regions? An in vitro and in vivo study. J Magn Reson Imaging. 2013;38:1103–10.
20. Pietrobon D, Moskowitz MA. Chaos and commotion in the wake of cortical spreading depression and spreading depolarizations. Nat Rev Neurosci. 2014;15:379–93.
21. Moskowitz CS, Welch ML, Jacobs MA, Kurland BF, Simpson AL. Radiomic analysis: study design, statistical analysis, and other bias mitigation strategies. Radiology. 2022;304:265–73.
22. Lin H, Liu Z, Yan W, Zhang D, Liu J, Xu B, Li W, Zhang Q, Cai X. Brain connectivity markers in advanced Parkinson's disease for predicting mild cognitive impairment. Eur Radiol. 2021;31:9324–34.
23. Yang J, Sui H, Jiao R, Zhang M, Zhao X, Wang L, Deng W, Liu X. Random-Forest-Algorithm-Based applications of the basic characteristics and serum and imaging biomarkers to diagnose mild cognitive impairment. Curr Alzheimer Res. 2022;19:76–83.
24. Tu Y, Zeng F, Lan L, Li Z, Maleki N, Liu B, Chen J, Wang C, Park J, Lang C, Yujie G, Liu M, Fu Z, Zhang Z, Liang F, Kong J. An fMRI-based neural marker for migraine without aura. Neurology. 2020;94:e741–51.
25. Yang H, Zhang J, Liu Q, Wang Y. Multimodal MRI-based classification of migraine: using deep learning convolutional neural network 08 information and computing sciences 0801 artificial intelligence and image processing. Biomed Eng Online. 2018;17:1–14.
26. Rocca MA, Harrer JU, Filippi M. Are machine learning approaches the future to study patients with migraine? Neurology. 2020;94:291–2.
27. Sun H, Chen Y, Huang Q, Lui S, Huang X, Shi Y, Xu X, Sweeney JA, Gong Q. Psychoradiologic utility of MR imaging for diagnosis of attention deficit hyperactivity disorder: A radiomics analysis. Radiology. 2018;287:620–30.
28. Fan L, Li H, Zhuo J, Zhang Y, Wang J, Chen L, Yang Z, Chu C, Xie S, Laird AR, Fox PT, Eickhoff SB, Yu C, Jiang T. The human brainnetome atlas: A new brain atlas based on connectional architecture. Cereb Cortex. 2016;26:3508–26.
29. Bonanno L, Lo Buono V, De Salvo S, Ruvolo C, Torre V, Bramanti P, Marino S, Corallo F. Brain morphologic abnormalities in migraine patients: an observational study. J Headache Pain. 2020;21:1–6.
30. Arca KN, VanderPluym JH, Halker Singh RB. Narrative review of neuroimaging in migraine with aura. Headache. 2021;61:1324–33.
31. Chou KH, Lee PL, Liang CS, Lee JT, Kao HW, Tsai CL, Lin GY, Lin YK, Lin CP, Yang FC. Identifying neuroanatomical signatures in insomnia and migraine comorbidity. Sleep. 2021;44:1–12.
32. Zhang J, Wu YL, Su J, Yao Q, Wang M, Li GF, Zhao R, Shi YH, Zhao Y, Zhang Q, Lu H, Xu S, Qin Z, Cui GH, Li J, Liu JR, Du X. (2017). Assessment of gray and white matter structural alterations in migraineurs without aura. The Journal of Headache and Pain. 2017;18:74.
33. Planchuelo-Gómez Á, García-Azorín D, Guerrero ÁL, Rodríguez M, Aja-Fernández S, de Luis-García R. Gray matter structural alterations in chronic and episodic migraine: A morphometric magnetic resonance imaging study. Pain Med. 2020;21:2997–3011.
34. Hu B, Yu Y, Dai YJ, Feng JH, Yan LF, Sun Q, Zhang J, Yang Y, Hu YC, Nan HY, Zhang XN, Zheng Z, Qin P, Wei XC, Cui GB, Wang W. Multi-modal MRI reveals the neurovascular coupling dysfunction in chronic migraine. Neuroscience. 2019;419:72–82.
35. Mayr A, Jahn P, Stankewitz A, Deak B, Winkler A, Witkovsky V, Eren O, Straube A, Schulz E. Patients with chronic pain exhibit individually unique cortical signatures of pain encoding. Hum Brain Mapp. 2022;43:1676–93.
36. Hougaard A, Nielsen SH, Gaist D, Puonti O, Garde E, Reislev NL, Iversen P, Madsen CG, Blaabjerg M, Nielsen HH, Krøigård T, Østergaard K, Kyvik KO, Madsen KH, Siebner HR, Ashina M. Migraine with aura in women is not associated with structural thalamic abnormalities. NeuroImage: Clin. 2020;28:102361.
37. Fu T, Liu L, Huang X, Zhang D, Gao Y, Yin X, Lin H, Dai Y, Wu X. (2022). Cerebral blood flow alterations in migraine patients with and without aura: An arterial spin labeling study. Journal of Headache and Pain. 2022;23:131.
38. Coppola G, Tinelli E, Lepre C, Iacovelli E, Di Lorenzo C, Di Lorenzo G, Serrao M, Pauri F, Fiermonte G, Bianco F, Pierelli F. Dynamic changes in thalamic microstructure of migraine without aura patients: a diffusion tensor magnetic resonance imaging study. Eur J Neurol. 2014;21:287–e13.
39. Torres-Ferrus M, Pareto D, Gallardo VJ, Cuberas-Borrós G, Alpuente A, Caronna E, Vila-Balló A, Lorenzo-Bosquet C, Castell-Conesa J, Rovira A, Pozo-Rosich P. Cortical metabolic and structural differences in patients with chronic migraine. An exploratory 18FDG-PET and MRI study. J Headache Pain. 2021;22:1–11.
40. Gaist D, Hougaard A, Garde E, Reislev NL, Wiwie R, Iversen P, Madsen CG, Blaabjerg M, Nielsen HH, Krøigard T, Østergaard K, Kyvik KO, Hjelmborg J, Madsen K, Siebner HR, Ashina M. Migraine with visual aura associated with thicker visual cortex. Brain. 2018;141:776–85.
41. Petrusic I, Dakovic M, Kacar K, Zidverc-Trajkovic J. Migraine with aura: Surface-based analysis of the cerebral cortex with magnetic resonance imaging. Korean J Radiol. 2018;19:767–76.
42. Wu D, Zhou Y, Xiang J, Tang L, Liu H, Huang S, Wu T, Chen Q, Wang X. Multi-frequency analysis of brain connectivity networks in migraineurs: a magneto-encephalography study. J Headache Pain. 2016;17(1).
43. Apkarian AV, Hashmi JA, Baliki MN. Pain and the brain: specificity and plasticity of the brain in clinical chronic pain. Pain. 2011;152(3 Suppl):S49–64.
44. Doan L, Manders T, Wang J. Neuroplasticity underlying the comorbidity of pain and depression. Neural Plast. 2015;504691.
45. Bannister K, Dickenson AH. The plasticity of descending controls in pain: translational probing. J Physiol. 2017;595:4159–66.
46. Fu T, Gao Y, Huang X, Zhang D, Liu L, Wang P, Yin X, Lin H, Yuan J, Ai S, Wu X. Brain connectome-based imaging markers for identifiable signature of migraine with and without aura. Quant Imaging Med Surg. 2024;14:194–207.

Publisher's note